A STUDY ON AIR POLLUTION BASED ON GEOSPATIAL ANALYSIS IN ULAANBAATAR CITY

Enkhjargal Natsagdorj[1], Gerelt-Od Munkhdii[3], Rentsendagva Dagva[2], Oyunbileg Erdenebadrakh[1], Usukhbayar Enkhjargal[3], Suvd-Erdene Dalkhaa[3]
[1]Department of Spatial Data Analysis, Centre for Policy Research and Analysis, Ulaanbaatar, Mongolia, Khangarid Palace, Sukhbaatar square, Baga toiruu-15160, Mongolia
Email: enkhjargal_spe@num.edu.mn; oyunbileg1208@gmail.com;

[2]Director, Centre for Policy Research and Analysis, Ulaanbaatar, Mongolia, Khangarid Palace, Sukhbaatar square, Baga toiruu-15160, Mongolia
Email: re.dagva@gmail.com;

[3]Department of System Dynamics Modelling, Centre for Policy Research and Analysis, Ulaanbaatar, Mongolia, Khangarid Palace, Sukhbaatar square, Baga toiruu-15160, Mongolia
Email: uskuenkhe32@gmail.com; odko.tf@gmail.com; suvderdene.aomg@gmail.com

KEY WORDS: Air pollution, EBK, Ger, MLR, Ulaanbaatar city

ABSTRACT: Air pollution is the main problem in Ulaanbaatar city, Mongolia. 45.1 percent of the total population of Ulaanbaatar city is affected by air pollution due to the concentration of coal-fired power plants, ger districts and vehicles in the capital. Due to extreme climatic conditions, high consumption of raw coal by people living in ger areas in the cold winter season, and increased population concentration, the air quality has reached the level of endangering human health. The goal of this study is to map air pollution in Ulaanbaatar city based on geospatial data analysis. Firstly, the global environmental monitoring index (GEMI) was calculated by near infrared and visible red spectral bands using Landsat OLI8 imagery. Secondly, automatic air quality monitoring stations (18 stations) were used for geostatistical interpolation (EBK) to determine the air pollution distribution. The study analysed the measured concentrations of Sulfur dioxide (SO2), Nitrogen dioxide (NO2), PM2.5, PM10 particles, and carbon monoxide (CO), the most harmful air pollutants to the human body. The results of the analysis are displayed that the average concentration of air pollutants in the cold season of 2022 from January to May in Ulaanbaatar city is 9μg/m3 or 8% of PM2.5 particles and 32μg/m3 of PM10 particles or 19%, nitrogen dioxide (NO2) is 3μg/m3 or 4% lower, while Sulfur dioxide (SO2) is 4μg/m3 or 3% higher than the same period of the previous year. Sulfur dioxide (SO2) pollution is high in industrial areas, and carbon monoxide (CO) pollution is highest in ger areas. Correlation analysis was performed for the air pollution in the Zaisan (apartment area) and Khailaast (ger areas) of Ulaanbaatar city based on actual data for the relationship between oxide (CO) Nitrogen dioxide (NO2), fine particles (PM2.5, PM10), Sulfur gas (SO2), Carbon dioxide and climate conditions (air pressure, temperature, air humidity, wind speed). Air pollution constituents in Zaisan area were positively related to air pressure and negatively related to temperature and wind speed from January 2022 to January 2023, but positively related (but weakly) to humidity. Overall, the present and previous situations of air pollution in the city have been reviewed and some solutions have been identified in this study.

1. INTRODUCTION

Air pollution is not only degrading the environment and causes real damage to infrastructure, but also air pollution particles matter (PM) negatively affects the quality of human life. The air quality of Ulaanbaatar city was measured into Sulfur dioxide (SO2), Nitrogen dioxide (NO2), Carbon monoxide (CO) and particulate matter (PM) 2.5, 10 particles in 18 stations around residential area. The Ulaanbaatar city's all citizens are affected by the air pollution which is the main problem. More than 50% of the citizens live in ger area where coal and wood are burned for heat (Amarsaikhan et al., 2014). Sources of air pollution consisted of thermal power plants 44.2%, ger areas 31%, auto vehicles 16.1%, and other 8.7 % by 2020. However, air pollution distributed from ger area of 55.6%, auto vehicles 28.9%, and others 15.5 % without thermal power plant (JICA, 2020). Through the air quality (AQ) monitoring network, which constitutes of the National Agency for Meteorology and Environmental Monitoring (NAMEM) and the Air Pollution Reduction Department of Ulaanbaatar city (APRD), a total of 18 stations are operating across the city (Soyol-Erdene et al., 2021).
The mean annual temperature measures -8 °C (northern areas) and 6 °C (southern regions) (Amarsaikhan et al., 2014). Because of the majority of the Mongolian climate situation, its air pollution is highly distributed by a long winter season (Sumiya et al., 2023). The World Health Organization (WHO) mentioned that air pollution of Ulaanbaatar city is the top 5 cities with worst air quality in the world (Guttikunda et al., 2013). International organizations and Mongolian governments taking actions for against the air pollution. For instance, Mongolian decision makers having an action for

the long-term on reducing auto vehicles emissions by systematically and re-planning of residential areas of ger area with high levels of air pollution (Sumiya et al., 2023). Therefore, this study aims to is to conduct geospatial data analysis on current situation of air pollution in Ulaanbaatar city. The objectives are listed as follows:

- To collect the air quality data between 2010 – 2023 and apply it for system dynamics modelling.
- To map air pollution based on air quality station's data on January 2022.
- To determine Global Environmental Monitoring Index (GEMI) using satellite images.
- To correlate air pollutants and field measurements

1.1 Study area

Study area is residential area of the Ulaanbaatar city which is covered central 6 districts (Songinokhairkhan, Chingeltei, Sukhbaatar, Bayanzurkh, Bayangol, Khan-Uul). There are 1.5 million people living in the area which is almost half of population (Figure 1, 2). It is in the north central part of Mongolia at an elevation about 1,300 meters and coldest capital city in the world. It has long winter and short summer season. The cold season starts in late October and ends in early April which continues for 140-150 days (Soyol-Erdene et al., 2021). People are living in the different types of houses which are yurt, house, apartments. Almost half of population lives in yurt and houses that we named ger area. They burn wood, coal in order to warm up their home.

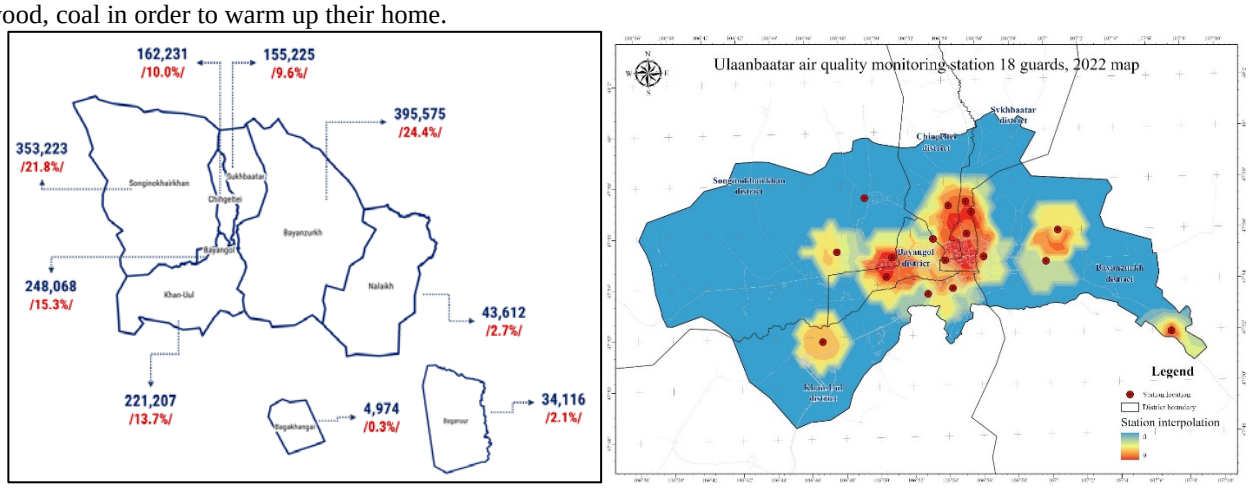

Figure 1. Ulaanbaatar city capital of Mongolia and residential area with the station's location

Figure 2. Ulaanbaatar city capital of Mongolia (winter photo)

2. DATA USED

2.1 Air pollution station data

There were 4 air quality monitoring stations, only two parameters were taken which are Sulfur dioxide (SO2), and Nitrogen dioxide (NO2), and the concentration was determined in the laboratory using chemical solutions until 2008 in the city. Now, there are 18 permanent air quality monitoring stations in Ulaanbaatar city, it identifies 2-6 types of

pollutants in the air. In 12 automatic monitors, Sulfur dioxide (SO2), Nitrogen dioxide (NO2), Carbon monoxide (CO), Ozone and particulate matter (PM) 2.5, 10 particles are continuously determined by automatic instruments every 15-30 minutes. These stations are placed depending on the population of the capital, the location of the air pollution source, and the land use. They are situated in ger areas, industrial areas, along the highways etc.

The Central Accredited Laboratory of Environmental Monitoring under the Ministry of Air Quality Council is responsible for the normal operation of the air quality monitoring equipments, and performs regular adjustments and inspections in accordance with the MNS 17025 standard of the environmental monitoring quality management system. In this study, the statistical data of 2010-2022 for 18 stations by air quality monitoring and analysis were used to make calculations for each year.

Table 1. Ulaanbaatar air quality monitoring station 18 stations, 2022

№	Station name	lat	Long	Determining indicators					
				SO_2	NO_x	CO	PM_{10}	$PM_{2.5}$	O_3
1	UB-01	47°53'38,44"	106°52'57,54"						
2	UB-02	47°54'55,46"	106°53'39,60"						
3	UB-03	47°55'04,73"	106°50'53,02"						
4	UB-04	47°55'02,65"	106°56'14,97"						
5	UB-05	47°55'58,45"	106°55'16,96"						
6	UB-07	47°54'20,22"	106°50'32,97"						
7	UB-08	47°51'57,43"	107°07'05,77"						
8	UB-11	47°57'05,15"	106°54'14,66"						
9	UB-12	47°57'14,50"	106°55'15,70"						
10	UB-13	47°53'50,44"	106°54'25,35"						
11	UB-14	47°56' 01"	107°00'37."45"						
12	UB-15	47°46'37.31"	107°15'9.18"						
13	Television	47°55'46.95"	106°53'19.08"						
14	Tolgoit	47°55'20.96"	106°47'41.37"						
15	Fly	47°51'50.25"	106°46'44.68"						
16	Amgalan	47°54'48.61"	106°59'52.59"						
17	Bayankhoshuu	47°57'27.12"	106°49'21.47"						
18	Dambadarjaa	47°56'49.29"	106°55'34.27"						

2.2 Landsat data

In this study, the Landsat OLI8 satellite image was combined for the enhancement of the Global Environmental Monitoring Index (GEMI) using near infrared and visible red spectral bands.

Landsat OLI8 satellite data

The Landsat 8 operational land imager (OLI) (January 2023) downloaded from the USGS earth resource observation and science (EROS) center website and applied it for this chapter.

Table 2. Landsat OLI spectral bands [1]

Landsat – 8 OLI & TIRS Bands (μm)		
30 m Coastal/Aerosol	0.435-0.451	I band
30 m Blue	0.452-0.512	II band
30 m Green	0.533-0.590	III band
30 m Red	0.636-0.673	IV band
30 m NIR	0.851-0.879	V band
30 m SWIR	1.566-1.651	VI band
100 m TIR	10.60-11.19	X band
100 m TIR	11.50-12.51	XI band
30 m SWIR	2.107-2.294	VII band
15 m Panchromatic	0.503-0.676	VIII band
30 m Cirrus	1.363-1.384	IX band

The Landsat 8 Operational Land Imager (OLI) and Thermal Infrared Sensor (TIRS) images consist of 9 spectral bands with a spatial resolution of 30 meters for the Bands 1 to 7 and 9. The ultra-blue Band 1 is useful for the coastal and aerosol studies. Band 9 is useful for the cirrus cloud detection. The resolution for Band 8 (panchromatic) is 15 meters. (Table 1) (U.S. Geological Survey, 2018). Additionally, in order to improve the satellite imagery and the impact of the atmospheric effects, we made an atmospheric correction to estimate the actual surface reflectance of each band. In this study, we applied visible red, near infrared bands of the Landsat images.

3. METHODOLOGY

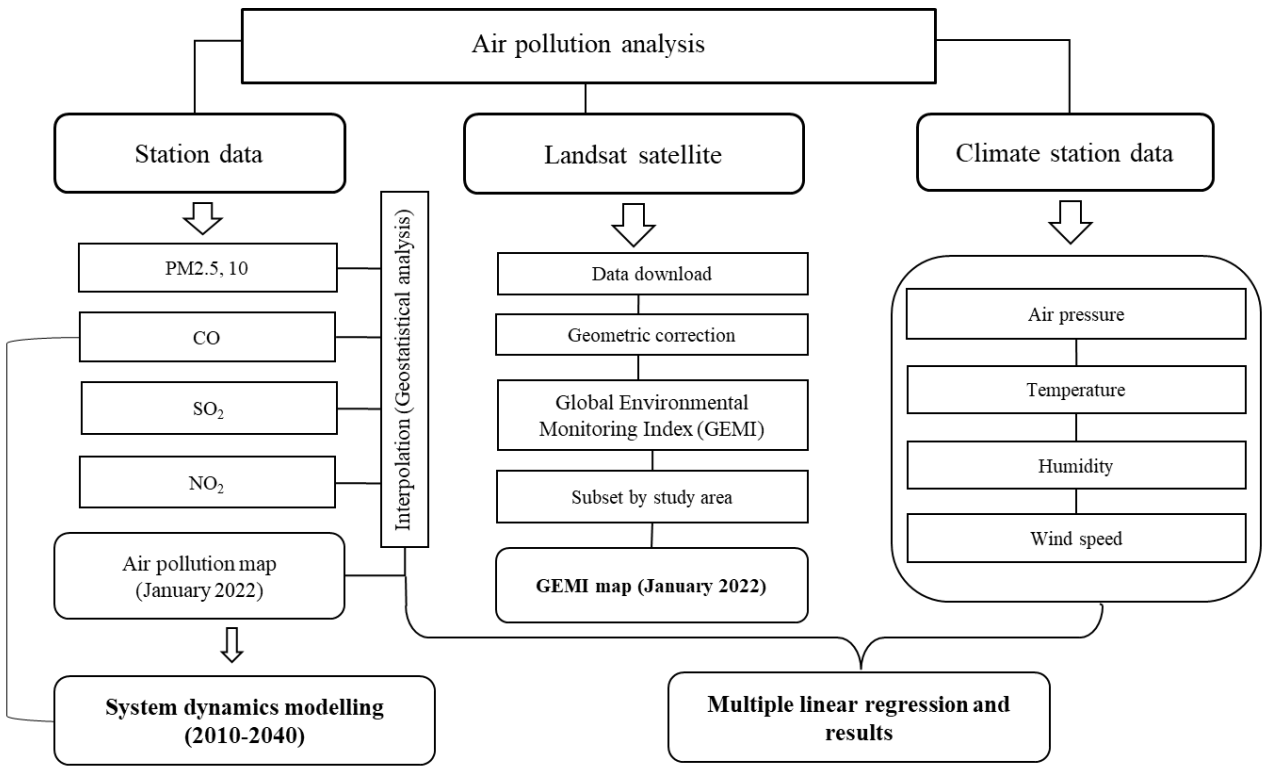

Schema 1. Methodology schema

Kriging interpolation method - The geostatistical analysis has been used as the main analytical tool to execute climatic and environmental factors and studies for relationships between soil moisture and environmental factors (Nyberg, 1996; Western et al., 1999). The Kriging interpolation method (Oliver & Webster, 1990; Yamamoto, 2005, 2007) was applied through ArcGIS to obtain a spatial distribution of the precipitation. The Kriging interpolation assumes that the distance or direction between the sample points reflects a spatial correlation that could be used to clarify the surface variation. The

[1] Source: http://landsat.usgs.gov/band_designations_landsat_satellites.php

Kriging method shows similarity with the IDW (Inverse Distance Weighted); it weighs the surrounding measured values to derive a prediction for an unmeasured location. The general formula for both interpolators is created as the weighed sum of the data, equation (1):

$$\hat{Z}(s_0) = \sum_{i=1}^{N} \lambda_i Z(s_i) \quad (1)$$

, where: $\boldsymbol{Z(s_i)}$ = the measured value at the i^{th} location

$\boldsymbol{\lambda_i}$ = an unknown weight for the measured value at the i^{th} location

$\boldsymbol{S_0}$ = the predicted location

$\boldsymbol{N}$ = the number of the measured values

In the IDW, the weight $\boldsymbol{\lambda_i}$ solely depends on the distance to the predicted location (Oliver & Webster, 1990). However, with the Kriging method, the weights are not only based on the distance between the measured points and the predicted location but also the overall spatial arrangement of the measured points. In order to use the spatial arrangement in the weights, the spatial autocorrelation must be quantified. Thus, in the ordinary Kriging method, the weight, $\boldsymbol{\lambda_i}$, depends on a fitted model to the measured points, the distance to the predicted location and the spatial relation among the measured values around the predicted location.

Global Environment Monitoring Index (GEMI) - Environmental monitoring is a crucial process for identifying and assessing the environmental impacts of human activities. With the help of GIS technology, it is possible to create a comprehensive Global Environmental Monitoring Index that provides a visual representation of the state of the environment. We will cover everything from data acquisition and processing to analysis and visualization. The Global Environmental Monitoring Index (GEMI) method is a nonlinear vegetation index for global environmental monitoring from satellite imagery. It is like NDVI, but it is less sensitive to atmospheric effects. It is affected by bare soil. Therefore, it is not recommended for use in areas of sparse or moderately dense vegetation (Pinty & Verstraete, 1992).

$$Xi = ((NIR\text{^}2 - Red\text{^}2) * 2 + (NIR * 1.5) + (Red * 0.5)) / (NIR + Red + 0.5) \quad (2)$$

$$GEMI = Xi * (1 - (Xi * 0.25)) - ((Red - 0.125) / (1 - Red)) \quad (3)$$

, where *NIR* is the near-infrared channel (0.772 ~ 0.898 μm) and (0.851 ~ 0.879 μm);
RED represents the visible red channels (0.631 ~ 0.692 μm) and (0.636 ~ 0.673 μm).

System dynamics modelling - System dynamics is grounded in control theory and the modern theory of nonlinear dynamics. System dynamics is also designed to be a practical tool that policy makers can use to help them solve the pressing problems they confront in their organizations. (D. Badarch, 2003) We applied system dynamic modeling for the air pollution dynamics in Ulaanbaatar city. The modelling was built by Mongolian language (Figure 3-6). It is provided many factors (vehicles by gas, diesel, petrol and electric, houses and yurts, residential area, weather condition, green area, thermal power plant, coal utilization, road and soil roads, etc).

The population of Ulaanbaatar is reached 1.65 million in 2022 and has average growth rate 2.5 percent. In 2040, population is expected to reach 2 million in city. The dynamic model of population growth is.

$$\frac{dP}{dt} = kP \quad (4)$$

$$P(t) = P_0 e^{kt} \quad (5)$$

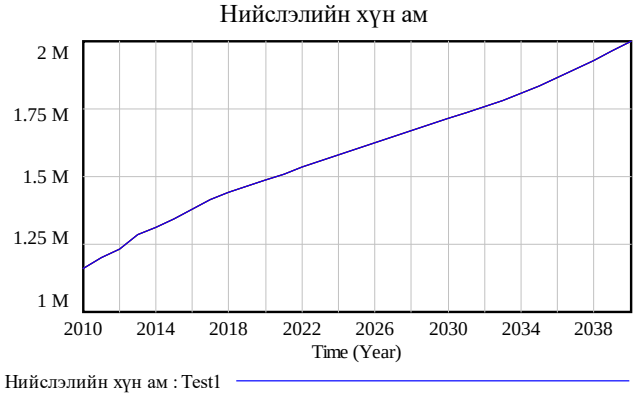

Figure 3. Population growth

Due to the growth of the city population, the average growth rate of vehicles is rising gradually over the years, namely 7 percent per year. As system dynamic modelling result, total number of vehicles is predicted to count at 1.25 million in 2040. Dynamic equation of vehicle growth is.

$$\frac{dM}{dt} = (\gamma \cdot P) - \sigma \cdot M \qquad (6)$$

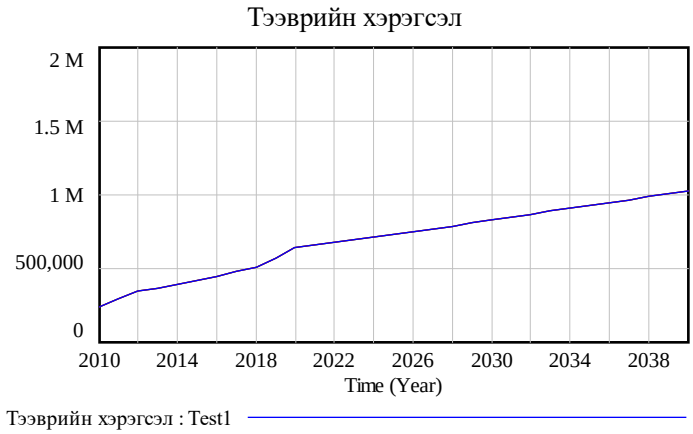

Figure 4. Auto vehicles growth

The total length of road network in Ulaanbaatar city is 1.8 percent per year. But this increment is less than the growth rate of vehicle, causing traffic congestion and exceeding the appropriate ratio of road capacity and vehicle number. Main impact of traffic congestion is decrease of average speed of car, relating to vehicle emissions.

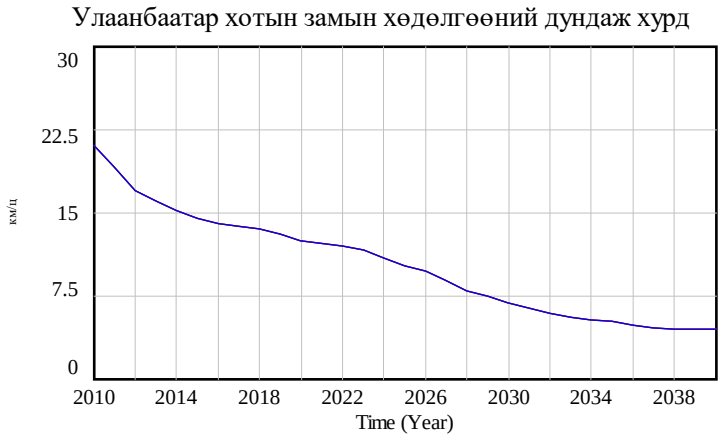

Figure 5. The average speed of traffic in Ulaanbaatar city

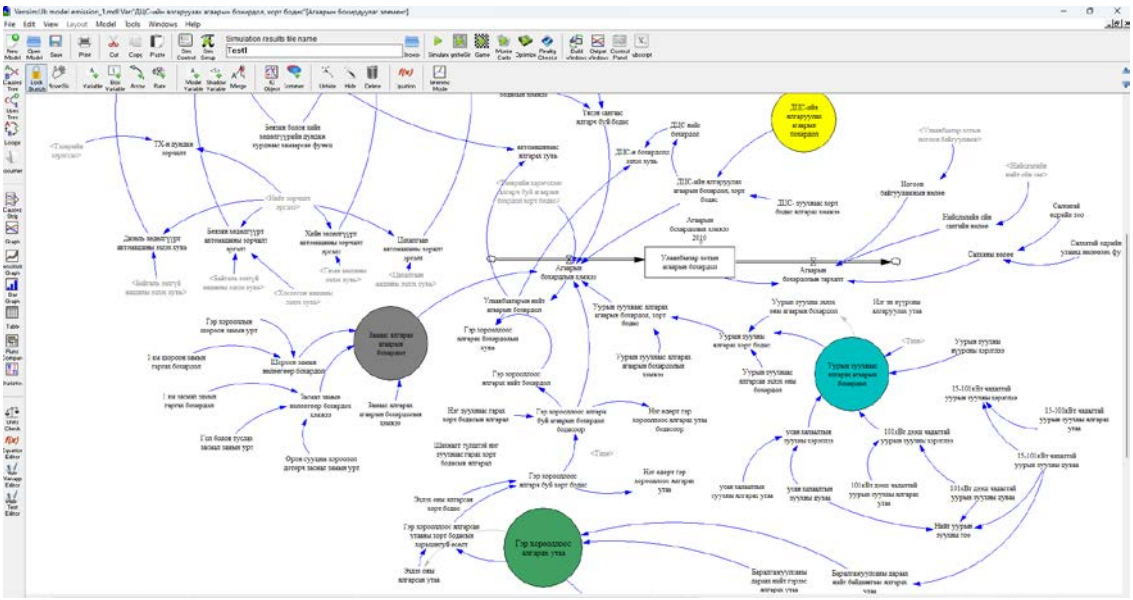

Figure 6. System dynamics modelling of the air pollution in Ulaanbaatar city.

Multi-regression soil moisture model - We assume that the air pollutants have been derived from air quality stations and that it depends on variables such as the air pressure, temperature, humidity, and wind speed. F represents the function of the dependent variables, as shown in equation (4).

Air pollutants =F (air pressure, temperature, humidity, wind speed) (4)

We selected therefore the multivariate regression analysis for this assumption. The multi-dimensional linear regression analysis could be described as:

$$y_i=\beta_0+\beta_1 x_{i1}+\beta_2 x_{i2}+\beta_3 x_{i3}+\beta_4 x_{i4}+\beta_5 x_{i5}+\epsilon \quad (5)$$

, where y_i is the observation variable that is the concentration of air pollutant elements; β_0 the intercept, β_1~β_5 represent the coefficients; x_i stands for the variables which are air pressure, temperature, humidity, and wind speed.

Pearson's correlation for the MI validation - The Pearson's correlation (r) was applied for the comparison between the air pollutants and climate conditions from the climate stations (equation 4). The equation of the coefficient of Pearson (r) is given in the following equation (2-4) (Sedgwick 2012):

$$r=\frac{\sum_{i=1}^{n}(X_i-\bar{X})(Y_i-\bar{Y})}{\sqrt{\sum_{i}^{n}(X_i-\bar{X})^2}\sqrt{\sum_{i}^{n}(Y_i-\bar{Y})^2}} \quad (4)$$

, where X_i and Y_i represent the individual derivations and measurements of the variables X and Y, respectively. $\bar{X}$ and $\bar{Y}$ demonstrate the means of X and Y, respectively (Sedgwick 2012). The linear Pearson's correlation (r) was determined on a monthly timescale (January 2021 – January 2023) for the derived air quality data and climatic data. Equation (4) was also utilized to investigate the relation between the estimated air pollution data and climate conditions.

4. ANALYSIS AND RESULTS

According to this study, first result was that we collected air quality monitoring data between 2010 and 2023. Then we applied system dynamics modelling for the Carbon monoxide (CO) until 2040. The results show that air pollution of ger area was decreasing by 46%, however auto vehicles pollutants are increasing by 48% until 2040 in Ulaanbaatar city (Figure 7).

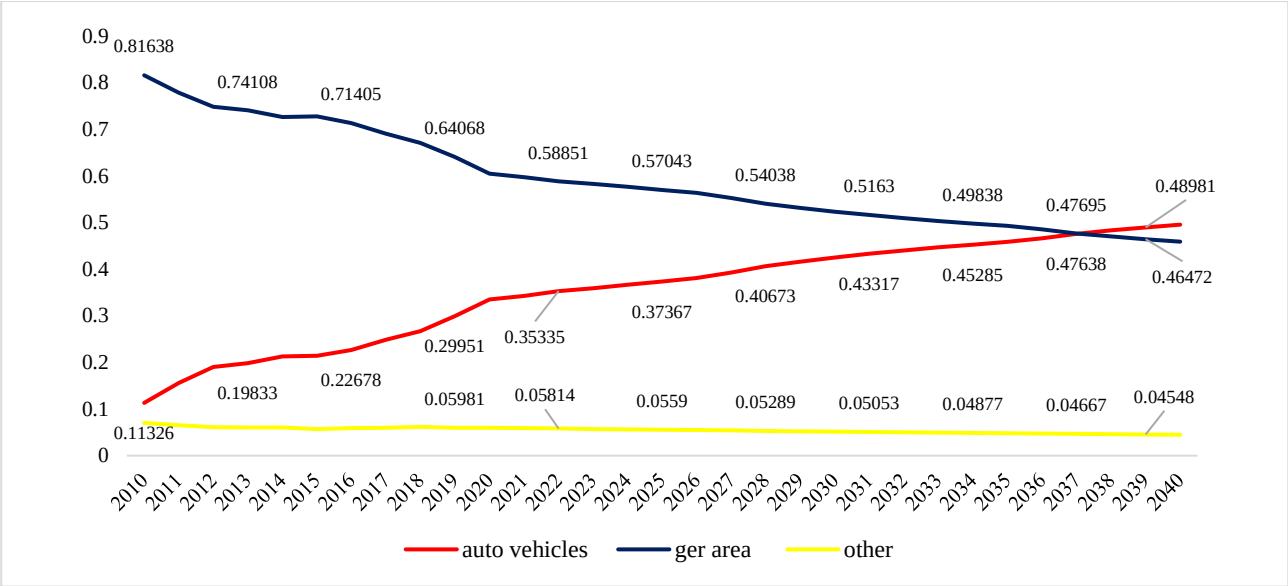

Figure 7. System dynamics modelling of the air pollution in Ulaanbaatar city.

The second result was determined to be the most polluted area in the city. The air pollution map was calculated by Kriging method of geostatistical analysis. The red color shows the highly polluted area, orange color represents moderate polluted area, yellow presents low polluted area and blue shows the clean air zone (Figure 8).

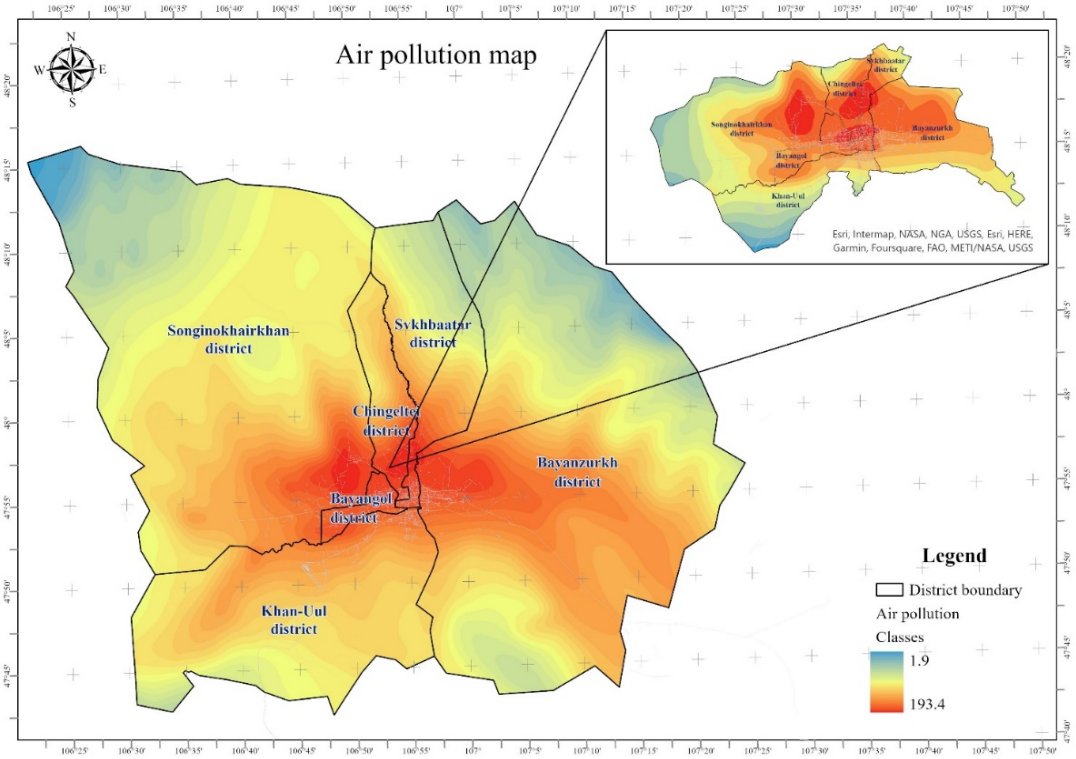

Figure 8. Air pollution map in 6 districts of Ulaanbaatar city

The 1.5 million people lives in north part of Ulaanbaatar city, rather 53% of people living in highest polluted area which represents with the red color (Figure 9).

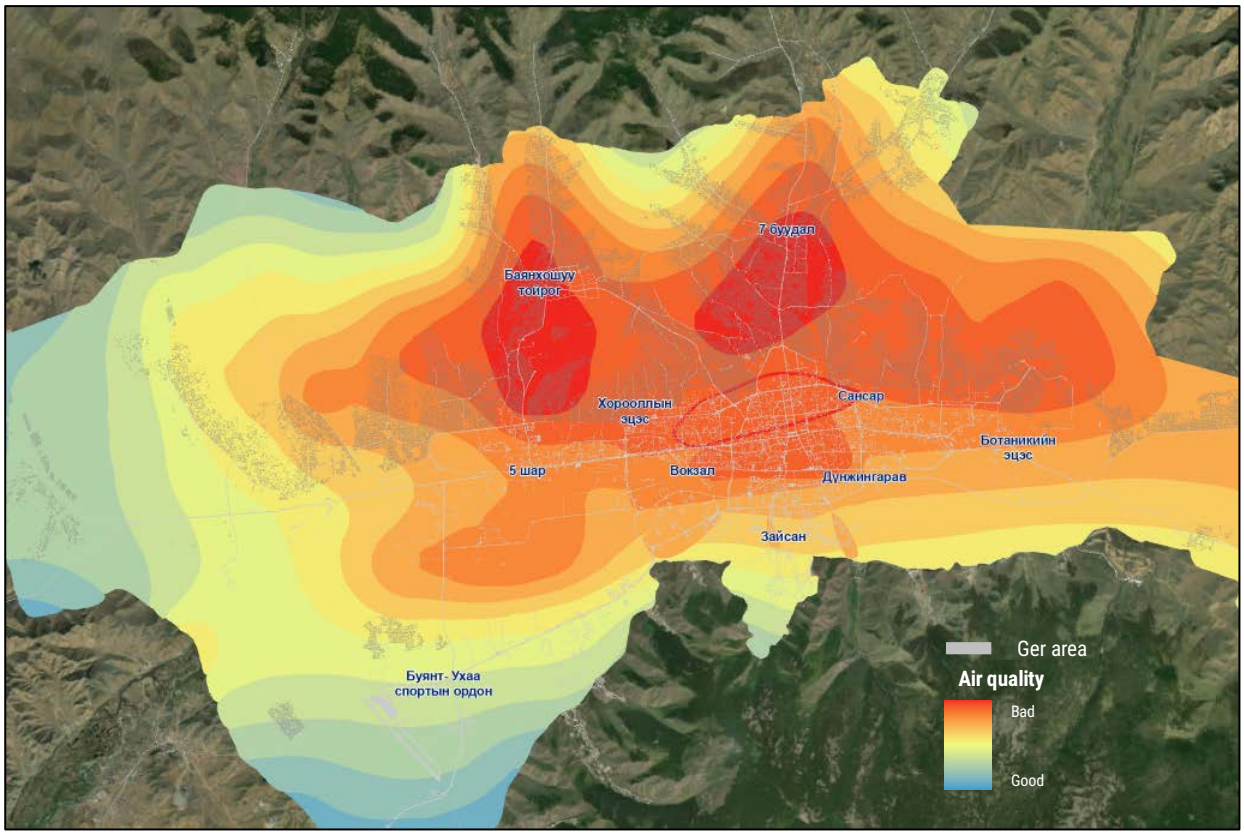

Figure 9. Air pollution map in 6 districts of Ulaanbaatar city

The third result was estimated GEMI based on visible red and near infrared spectral bands of Landsat OLI8 images. GEMI is identifying and assessing the environmental impacts of human activities. The GEMI values are represented to a range between 0 and 200, of which values over 100 display the highly effected and values approaching to one show a low effected by human activities (Figure 10).

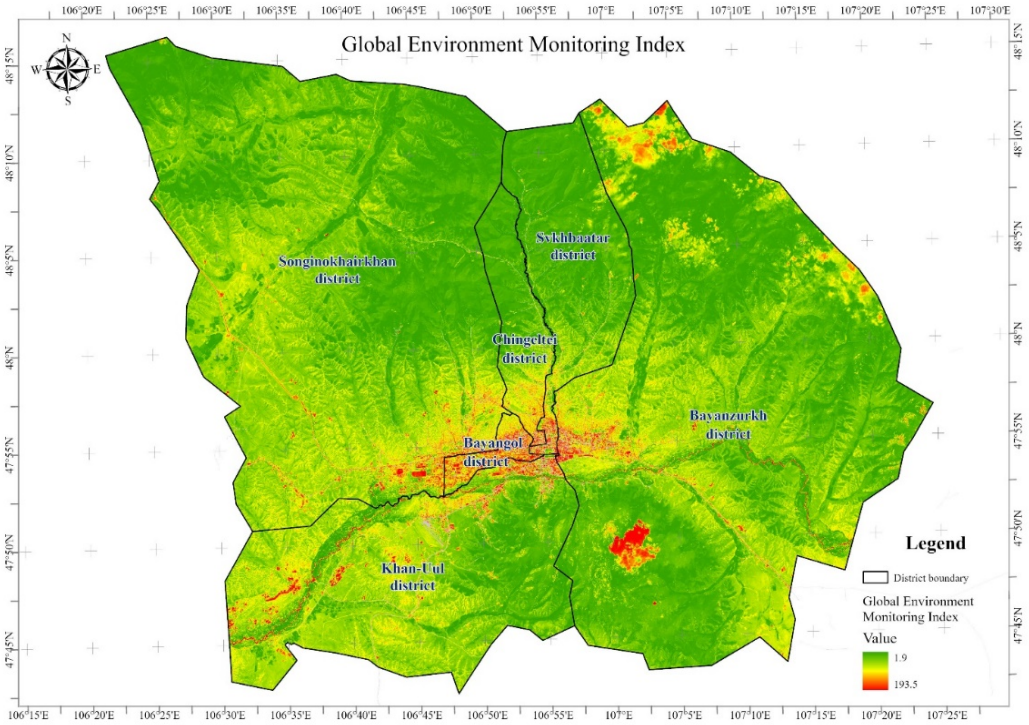

Figure 10. Global Environmental Monitoring Index map of Ulaanbaatar city (January 2023)

The fourth result shows that overlapped all high polluted areas in the city on GEMI map. Figure 7 displays high affected area displays in red color which is 90 percent of ground data (Figure 11).

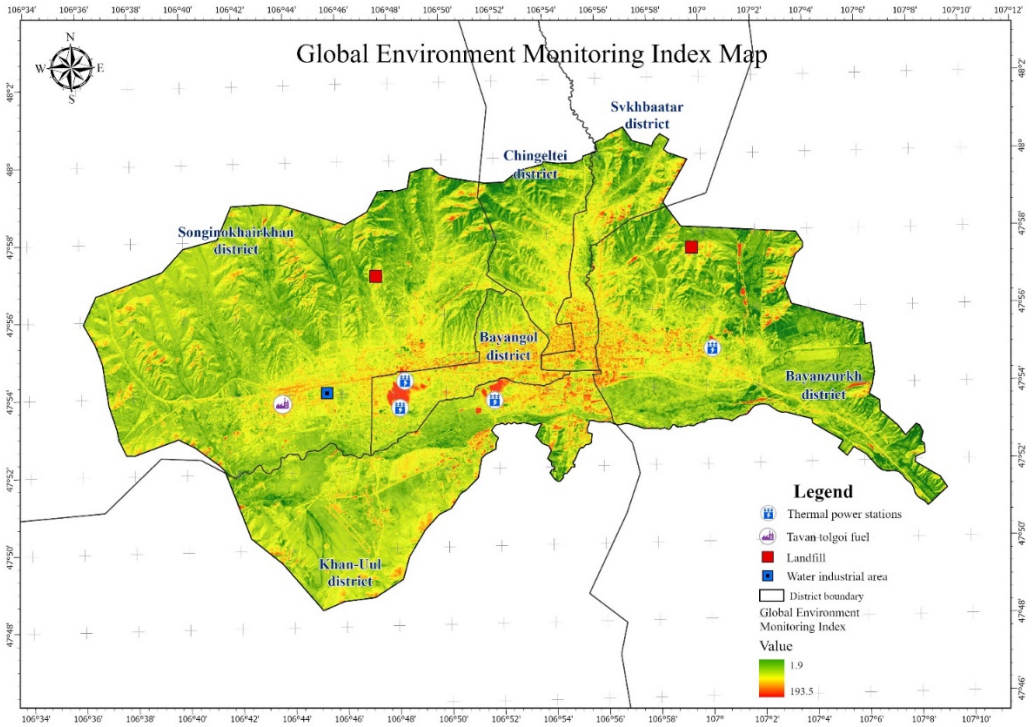

Figure 11. Overlapped industrial areas on GEMI map (January 2023)

Lastly, we selected two locations which were the highest pollution area (Khailaast ger area) and lowest pollution area (Zaisan apartment area). The constituent elements of air pollution in Zaisan from January 2021 to January 2023 were positively related to air pressure, negatively related to temperature and wind speed, and positively related (but weakly) to humidity (Table 3).

Table 3. Correlation between air pollution and climatic conditions in Zaisan (apartment area)

	NO_2	PM10	PM2.5	SO_2	CO
Air pressure	0.2005	0.0168	0.1673	0.0392	0.2806
Temperature	**-0.4064**	-0.2512	**-0.4742**	-0.18	**0.5953**
Humidity	0.1453	-0.0712	0.13	0.0036	0.2356
Wind speed	-0.327	-0.0244	0.0794	-0.0143	-0.2636

The concentration of NO_2, PM10, PM2.5, SO_2, and CO in the air increases when the air pressure increases from January 2021 to January 2023, while the concentration of pollutants decreases when the temperature and wind speed increase. Compared to Zaisan, there is a high correlation between the 5 constituent elements of air pollution and the climatic conditions (Table 4).

Table 4. Correlation between air pollution and climatic conditions in Khailaast (ger area)

	NO_2	PM10	PM2.5	SO_2	CO
Air pressure	0.3178	0.1537	0.2233	**0.4422**	0.3281
Temperature	**-0.7112**	**-0.4838**	**-0.5051**	**-0.6381**	**0.5953**
Humidity	0.0846	0.0316	0.1369	0.1405	0.212
Wind speed	**-0.4978**	-0.3404	-0.308	-0.4134	**-0.5178**

When temperature is constant, air pressure and relative humidity are negatively correlated with five air pollution constituents (NO_2, PM10, PM2.5, SO_2 and CO), while only PM10 is positively correlated with wind speed (0.022) (Table 5). It can be concluded that when the temperature is constant, the concentration of substances such as NO2, PM2.5, PM10, SO2, and CO in the air decreases with the increase in air pressure and relative humidity, and the increase in wind speed increases the concentration of PM10 particles.

Table 5. Correlation between air pollution and climatic conditions in Zaisan (apartment area)

Constant		NO2	PM10	PM2.5	SO2	CO
Temperature	Air pressure	-0.00185	-0.149	-0.112	-0.151	-0.056
	Humidity	-0.00844	-0.167	-0.038	-0.164	0.057
	Wind speed	-0.282	**0.022**	0.00106	0.001129	-0.212

However, when the temperature is constant in the air, the concentration of other substances decreases when the air pressure, humidity, and wind speed increase, while the concentration of carbon monoxide (CO) increases when the humidity increases.

Table 5. Correlation between air pollution and climatic conditions in Khailaast (ger area)

Constant		NO2	PM10	PM2.5	SO2	CO
Temperature	Air pressure	-0.09	-0.116	-0.047	0.248	-0.032
	Humidity	-0.091	-0.022	-0.029	-0.031	**0.075**
	Wind speed	-0.418	-0.248	-0.223	-0.316	-0.446

5. DISCUSSION

Air pollution of Ulaanbaatar city is the main problem in Mongolia. It is rapidly increasing last 2 decades due to new settlement area and increasing number of auto vehicles. Ulaanbaatar's power plant and small boilers use 4.0 million tons, households use more than 400,000 tons of coal, and more than 300,000 square meters of wood, and more than 700,000 cars continue to pollute the air and soil with smoke, soot, and ash (MEC, 2004). About the GEMI, reflectance measurements in the visible and near-infrared regions have been analysed with simple but powerful indices designed to enhance the contrast between the vegetation and other surface types, however, these indices are sensitive to atmospheric effects (Pinty & Verstraete, 1992).

In this study, if we do not take actions on against air pollution then auto vehicles 49% in the Ulaanbaatar city. Most polluted area is located around the industrial area. The result was 90 percent of factories (thermal power plant, landfill, tavan tolgoi fuel, water treatment plant) are overlayed in the worst GEMI map.

We compared air pollutants and climate conditions. Correlation analysis was performed for the air pollution in the Zaisan (apartment area) and Khailaast (ger areas) of Ulaanbaatar city based on actual data for the relationship between oxide (CO) Nitrogen dioxide (NO2), fine particles (PM2.5, PM10), Sulfur gas (SO2), Carbon dioxide and climate conditions (air pressure, temperature, air humidity, wind speed). Air pollution constituents in Zaisan area were positively related to air pressure and negatively related to temperature and wind speed from January 2022 to January 2023, but positively related (but weakly) to humidity.

In the end, air pollution represents a main threat to public health in Ulaanbaatar city and control efforts' primary focus should be in ger area and auto vehicles in the future.

5.1 Acknowledgements

The authors are very grateful to provide the data for the National Agency for Meteorology and Environmental Monitoring (NAMEM) and the Air Pollution Reduction Department of Ulaanbaatar city (APRD).

5.2 References

Amarsaikhan, D., Battsengel, V., Nergui, B., Ganzorig, M., & Bolor, G. (2014). A Study on Air Pollution in Ulaanbaatar City, Mongolia. *Mongolia. Journal of Geoscience and Environment Protection*, *2*, 123–128. https://doi.org/10.4236/gep.2014.22017

JICA. (2020). *Capacity Development Project for Air Pollution Control in Ulaanbaatar City | Mongolia | Countries & Regions | JICA*. JICA. https://www.jica.go.jp/Resource/mongolia/english/activities/activity17.html

D. Badarch, B. O. A. E.-A. (2003). *Principles of system dynamics modeling* (Vol. 1).

Guttikunda, S. K., Lodoysamba, S., Bulgansaikhan, B., & Dashdondog, B. (2013). Particulate pollution in Ulaanbaatar, Mongolia. *Air Quality, Atmosphere and Health*, *6*(3), 589–601. https://doi.org/10.1007/S11869-013-0198-7/METRICS

Nyberg, L. (1996). Spatial variability of soil water content in the covered catchment at Gårdsjön, Sweden. *Hydrological Processes*, *10*(1), 89–103. https://doi.org/10.1002/(SICI)1099-1085(199601)10:1<89::AID-HYP303>3.0.CO;2-W

Oliver, M. A., & Webster, R. (1990). Kriging: A method of interpolation for geographical information systems. *International Journal of Geographical Information Systems*, *4*(3), 313–332. https://doi.org/10.1080/02693799008941549

Pinty, B., & Verstraete, M. M. (1992). GEMI: a non-linear index to monitor global vegetation from satellites. *Vegetatio*, *101*(1), 15–20. https://doi.org/10.1007/BF00031911/METRICS

Soyol-Erdene, T. O., Ganbat, G., & Baldorj, B. (2021). Urban Air Quality Studies in Mongolia: Pollution Characteristics and Future Research Needs. *Aerosol and Air Quality Research*, *21*(12), 210163. https://doi.org/10.4209/AAQR.210163

Sedgwick, P. 2012. “Pearson’s Correlation Coefficient.” *BMJ (Online)*. British Medical Journal Publishing Group. https://doi.org/10.1136/bmj.e4483.

Sumiya, E., Dorligjav, S., Purevtseren, M., Gombodorj, G., Byamba-Ochir, M., Dugerjav, O., Sugar, M., Batsuuri, B., & Tsegmid, B. (2023). Climate Patterns Affecting Cold Season Air Pollution of Ulaanbaatar City, Mongolia. *Climate*, *11*(1), 4. https://doi.org/10.3390/CLI11010004/S1

U.S. Geological Survey. (2018). Landsat Collections. *Fact Sheet*, *August*, 2. https://doi.org/10.3133/fs20183049

Western, A. W., Grayson, R. B., Blöschl, G., Willgoose, G. R., & McMahon, T. A. (1999). Observed spatial organization of soil moisture and its relation to terrain indices. *Water Resources Research*, *35*(3), 797–810. https://doi.org/10.1029/1998WR900065

Yamamoto, J. K. (2005). Correcting the smoothing effect of ordinary kriging estimates. *Mathematical Geology*, *37*(1), 69–94. https://doi.org/10.1007/s11004-005-8748-7

Yamamoto, J. K. (2007). On unbiased backtransform of lognormal kriging estimates. *Computational Geosciences*, *11*(3), 219–234. https://doi.org/10.1007/s10596-007-9046-x